Biophysical Journal Volume 66 March 1994 554–560

TEACHING BIOPHYSICS

Teaching Active Transport At the Turn of the Twenty-First Century: Recent Discoveries and Conceptual Changes

Giuseppe Inesi
Department of Biological Chemistry, University of Maryland School of Medicine, Baltimore, Maryland 21201 USA

ABSTRACT The conceptual advances introduced by recent discoveries in the field of active transport have triggered a transition from a "black box" approach to a "mechanistic" approach. At present, treating this subject in the graduate setting requires consideration of equilibrium and kinetic experimentation, protein chemistry, mutational analysis and molecular structure, with the aim of defining the "transport machine."

INTRODUCTION

Concentration of solutes in membrane bound compartments (i.e., active transport) is an extremely important function in biology, as it provides substrates where metabolically needed, regulates osmotic phenomena, and makes possible transmembrane electrical signalling. The work of moving solutes against a concentration gradient requires energy which is often supplied by a coupled chemical reaction (e.g., ATP hydrolysis). In turn, the free energy stored as a transmembrane gradient can be utilized to accomplish chemical work (e.g., ATP synthesis). I wish to give here a broad discussion of how recent discoveries, obtained through a variety of methodological approaches, have extended our view of active transport from a phenomenological approach to an understanding of pertinent protein structures and coupling mechanisms.

Active transport has been commonly presented in terms of the free energy required to form a transmembrane gradient, as in

$$\Delta G = RT\ln([A_2]/[A_1]) + zF\Delta V \qquad (1)$$

where A_1 and A_2 stand for the concentrations of the solute to be transported from compartment 1 to compartment 2, z for the electrical charge of the transported species, R for the gas constant, T for the absolute temperature, and F for the Faraday constant. This relationship applies, for instance, to the simple case of membrane bound cation pumps. Conversely, the free energy derived from transmembrane electrochemical gradients has been presented in analogous terms, such as the "proton-motive force" which is utilized for ATP synthesis in mitochondria. Matching these gradient-related "free energies" with the chemical potentials of coupled reactions, and establishing the stoichiometry of coupling, have been dominant concerns during the fifth and sixth decades of this century. This approach, however, has shed little light on the mechanism of energy transduction, as Eq. 1 is a "black box" from the mechanistic point of view. In recent years, however, purification and cloning of membrane-bound transport ATPases, characterization of their partial reactions, and elucidation of protein structure and function have produced a large body of information and new ideas. I will use the Ca^{2+} pump (Hasselbach, 1964) as an example in my discussion, as this pump involves primarily a single protein and is relatively well characterized.

Description of experimental systems and functional parameters

It is of definite advantage to present an experimental system which permits convenient measurements of both enzyme activity and coupled transport function under the same conditions. Vesicular fragments of longitudinal sarcoplasmic reticulum (SR) can be isolated with good yield by differential centrifugation of muscle homogenates. The isolated SR vesicles contain a high density of Ca^{2+} pump units, homogeneously oriented with respect to the membrane plane (Fig. 1).

Each pump unit is made of a single 110-kDa polypeptide chain corresponding to a Ca^{2+}-dependent ATPase molecule. The ATPase accounts for 50–60% of the total protein associated with the vesicles, and sustains high rates of ATP utilization coupled to Ca^{2+} transport. Under favorable conditions two calcium ions are transported into the lumen of the vesicles per ATP utilized by the ATPase.

Due to the high density of pump units and the relatively small volume of the native vesicles, Ca^{2+} in the lumen reaches the millimolar concentration range a few seconds after the addition of ATP, resulting in inhibition of further transport. Alternatively, prolonged steady state activity can be obtained by reconstituting the Ca-ATPase in proteoliposomes with a lower protein/lipid ratio (Levy et al., 1990). Thereby, the ATPase density within the membrane plane is

Received for publication 20 September 1993 and in final form 8 December 1993.

Address reprint requests to Giuseppe Inesi at the Department of Biological Chemistry, University of Maryland School of Medicine, Baltimore, MD 21201.

© 1994 by the Biophysical Society

0006-3495/94/03/554/07 $2.00

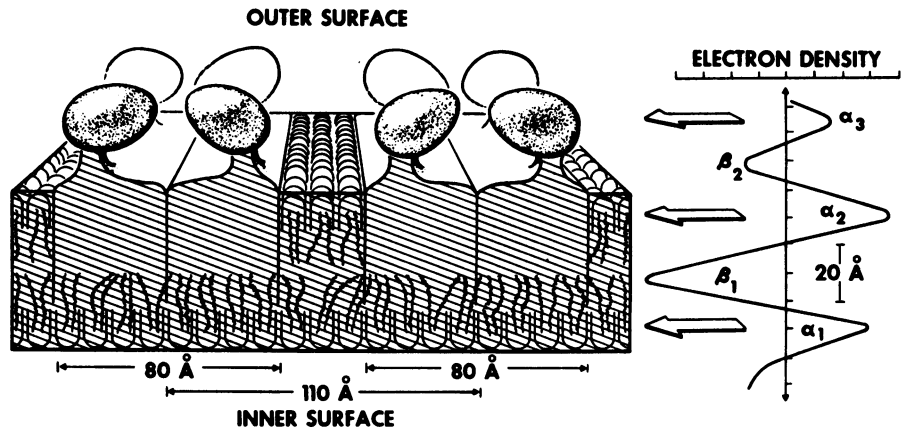

FIGURE 1 Diagrammatic assembly of ATPase molecules within the SR membrane. The diagram shows the dense distribution of ATPase molecules within the membrane. The shape of each ATPase, derived from direct electron microscopic observations, includes an oval-shaped head connected through a stalk to a membrane-bound region (Inesi, 1979). A matching (*top, right*) electron density profile along the axis perpendicular to the plane of the membrane was derived from low angle x-ray diffraction (Dupont et al., 1973).

lower. Another advantage is the very low electrolyte leak in the reconstituted proteoliposomes. In this system, ATP-dependent Ca^{2+} uptake proceeds for several minutes before inhibitory concentrations of lumenal Ca^{2+} are reached. Inward Ca^{2+} transport is accompanied by H^+ countertransport with a 1:1 stoichiometric ratio and, owing to the unbalanced charge transfer, the pump is electrogenic. Although it is uncertain whether countertransport involves direct exchange of H^+ for Ca^{2+} on the same protein acidic residues or proceeds through independent pathways, the overall catalytic and transport cycle may be written as:

$$ATP + 2Ca^{2+}_{out} + 2H^+_{in} \leftrightharpoons ADP + P_i + 2Ca^{2+}_{in} + 2H^+_{out} \quad (2)$$

It is useful to point out that development of transmembrane electrical potential is related to net charge transfer by the pump according to:

$$dV/dt = (dQ/dt)\,(1/C_m), \quad (3)$$

where dV/dt is the rate of change of the transmembrane voltage, dQ/dt the rate of charge transfer per unit membrane area, and C_m the capacitance per unit membrane area ($\sim 1\ \mu F\ cm^{-2}$). It is possible to match, based on Eq. 3, the experimentally observed initial rates of voltage development with the initial rates of Ca^{2+} transport and H^+ countertransport. In fact, considering a rate of Ca^{2+} uptake of 1.4×10^{-9} mol/mg protein s^{-1} at 12°C and correcting by the Avogadro number (6.022×10^{23}) we obtain a transport rate of 8.4×10^{14} molecules of Ca^{2+}/mg protein s^{-1}. Since 1 mg of protein corresponds to 10^5 cm^2 of proteoliposomal membrane area, we can write 8.4×10^9 molecules of Ca^{2+} cm^{-2} s^{-1}. If we now consider that 1 Ca^{2+} carries 1 net charge (due to H^+ countertransport), and that e_o (elementary particle, or "coulombic equivalent of charge") is 1.6×10^{-19} coulomb, the final estimate of charge transfer is

$$dQ/dt = 1.3 \times 10^{-9}\ \text{coulomb cm}^{-2}\ \text{s}^{-1}, \quad (4)$$

which divided by 1×10^{-6} F cm^{-2}, yields

$$dV/dt = 1.3\ mV\ s^{-1} \quad (5)$$

This is very close to the experimentally observed value, and is consistent with the independently observed stoichiometry of 1 Ca^{2+} transported versus 1 H^+ countertransported. The experimental parameters considered for this analysis should be actual rates of net transport and countertransport rather than ATPase activity, since the latter introduces errors related to uncoupled cycles. Although assumptions made for these calculations may preclude very accurate determinations of charge transfer per cycle, it is clear that the electrogenic behavior of the pump, as evidenced by its voltage development, requires countertransport of fewer than 2 H^+ per Ca^{2+}. A detailed treatment of electrogenic pumps can be found in a recent book by Peter Lauger (1991).

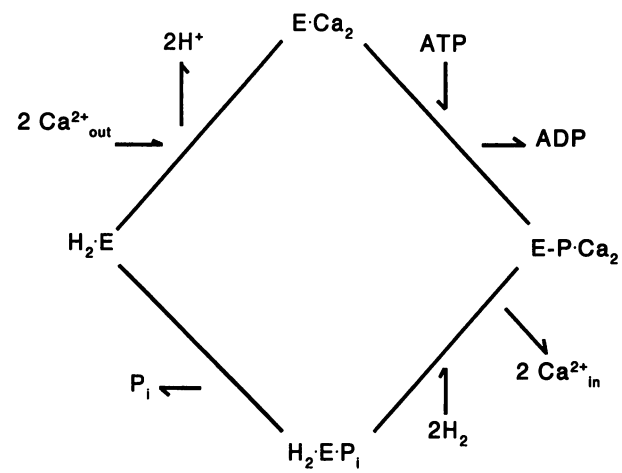

FIGURE 2 Diagram of a Ca^{2+} ATPase reaction scheme. The diagram shows the simplest possible sequence for Ca^{2+} binding and enzyme activation, ATP utilization and formation of a phosphorylated enzyme intermediate, inward displacement of bound Ca^{2+}, and hydrolytic cleavage of the intermediate.

The catalytic cycle and its partial reactions

While proteoliposomes reconstituted with low protein to lipid ratios yield convenient systems for steady state experimentation, native SR vesicles present a distinctive advantage in equilibrium or presteady state experiments designed to characterize the partial reactions of the catalytic and transport cycle. This is because the high density of ATPase units yields

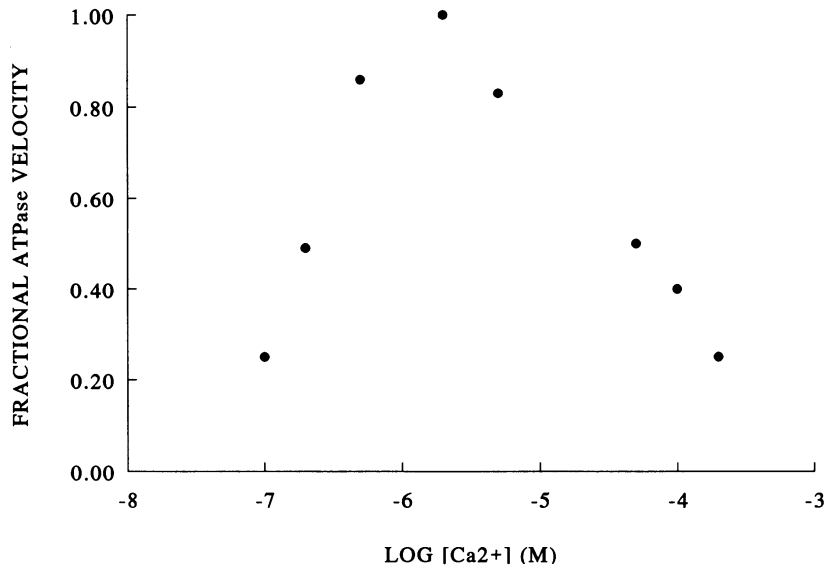

FIGURE 3 Ca^{2+} concentration range of effective ATPase kinetics. The steady state velocity of SR ATPase is here plotted as a function of Ca^{2+} concentration. The experiment was performed with SR vesicles rendered leaky with a Ca^{2+} ionophore, thereby preventing formation of a gradient and exposing the Ca^{2+} binding sites of outward or inward orientation to the same concentration of Ca^{2+}. The resulting bell shaped curve illustrates that, within due approximations, the pump is activated cooperatively by Ca^{2+}_{out} in the micromolar range, and inhibited by Ca^{2+}_{in} in the 0.1–1.0 mM range.

measurable concentrations of enzyme intermediates. In fact, the experimental evidence indicates that the ATPase must bind Ca^{2+} to be activated, and then utilizes ATP through formation of a phosphorylated intermediate. The bound Ca^{2+} is then released into the lumen of the vesicles, and the phosphoenzyme undergoes hydrolytic cleavage as briefly outlined in Fig 2.

It is then possible to consider a minimal number of partial reactions, and their measured equilibrium constants, as follows:

$$H_2E + 2Ca^{2+}_{out} \rightleftharpoons E{\cdot}Ca_2 + 2H^+_{out} \qquad (3 \times 10^{12}\ M^{-2})$$

$$E{\cdot}Ca_2 + ATP \rightleftharpoons ATP{\cdot}E{\cdot}Ca_2 \qquad (1 \times 10^5\ M^{-1})$$

$$ATP{\cdot}E{\cdot}Ca_2 \rightleftharpoons ADP{\cdot}E{\text{-}}P{\cdot}Ca_2 \qquad (0.3)$$

$$ADP{\cdot}E{\text{-}}P{\cdot}Ca_2 \rightleftharpoons E{\text{-}}P{\cdot}Ca_2 + ADP \qquad (7 \times 10^{-4}\ M)$$

$$E{\text{-}}P{\cdot}Ca_2 + 2H^+_{in} \rightleftharpoons H_2E{\text{-}}P + 2Ca^{2+}_{in} \qquad (3 \times 10^{-6}\ M^2)$$

$$H_2E{\text{-}}P \rightleftharpoons H_2E{\cdot}P_i \qquad (1)$$

$$H_2E{\cdot}P_i \rightleftharpoons H_2E + P_i \qquad (1 \times 10^{-2}\ M),$$

where the equilibrium constants relate to conditions allowing constant temperature (25°C) and pH (7.0). A detailed account of experimentation and analysis used for equilibrium and kinetic characterization of these partial reactions can be found in Inesi et al. (1988).

In the reaction sequence given above, the initial high affinity acquisition (reaction 1) of two Ca^{2+} from the outer medium activates the enzyme, permitting utilization of ATP and formation of a phosphorylated intermediate (reactions 2–4). In turn, enzyme phosphorylation destabilizes and changes the vectorial orientation of the bound Ca^{2+}, thereby increasing the probability of its dissociation into the lumen of the vesicles (reaction 5). Note that the equilibrium constant for the enzyme phosphorylation by ATP is nearly 1, indicating that the free energy of ATP is conserved by the enzyme, and utilized to change the Ca^{2+} binding characteristics. Finally, the phosphoenzyme undergoes hydrolytic cleavage and releases P_i (reactions 6 and 7) before entering another cycle. The reaction sequence shows clearly that the *direct mechanistic device for cation translocation against a gradient is enzyme phosphorylation, rather than hydrolytic cleavage of P_i* (Inesi et al., 1978).

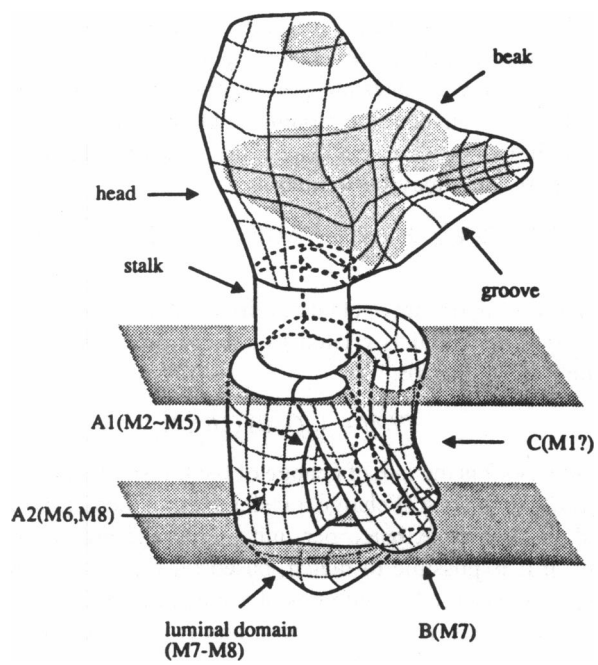

FIGURE 4 Three-dimensional image of the SR ATPase obtained by cryoelectron microsopy. One of the membrane-bound ATPase molecules shown in Fig. 1 is here presented with its three-dimensional structure at 14-Å resolution (Toyoshima et al., 1993). The extramembranous cytosolic region is here shaped as a head with a beak, still connected through a stalk to the 10 membrane-spanning helices which are tentatively identified with their number.

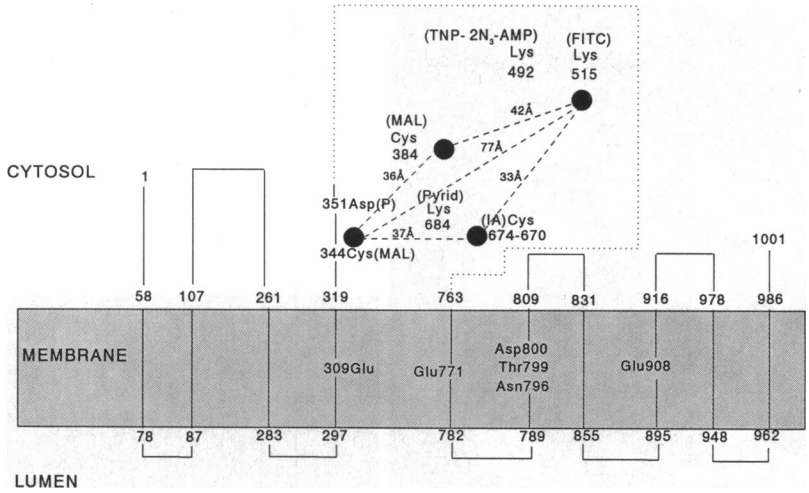

FIGURE 5 Topology of the ATPase sequence with respect to the SR membrane. The distribution of the sequence is based on the original assignment of MacLennan et al. (1985) as modified by Clarke et al. (1989a,b). The amino and carboxyl termini are both placed on the cytosolic side. A small and a large cytosolic loop are comprised between residues 107 and 261, and 319 and 763, respectively. These two loops constitute the head and stalk shown in Fig 4. Within the cytosolic region, note that Asp^{351} is the residue undergoing phosphorylation by ATP for formation of the catalytic intermediate. Specific points of reference for spectroscopic estimates of distances in the cytosolic region (Bigelow and Inesi, 1992) are shown in black circles. Lys^{492} which is reactive to an azido group in the adenosine moiety of ATP, and Lys^{684} which is reactive to a pyridoxal group at the phosphorylated end of ATP, are shown also in the cytosolic region in proximity to the appropriate distance reference point. The membrane bound region includes the 10 putative spanning helices and the six residues involved in Ca^{2+} binding functions.

As the catalytic and transport cycle is likely to include isomeric transitions (e.g., E_1 to E_2, and/or possibly others) in addition to the chemical reactions listed above, it should be noted that such transitions are coupled implicitly with the chemical reactions subjected to experimental measurement, and their influence is reflected by the equilibrium constants given above. In fact, the standard free energies ($-RT\ln K$) of the partial reactions add up to the standard free energy of ATP hydrolysis (γ-phosphate), as expected. Most interestingly, the standard free energy diagram for the partial reactions reveals that the chemical potential of ATP does not manifest itself in the phosphoryl transfer or hydrolytic cleavage reactions (K_4 and K_6 near 1), but rather in the drastic reduction of the enzyme affinity for Ca^{2+} (compare K_1 to $1/K_5$). We can then write that, under standard conditions

$$\Delta G = nRT \ln (K_a^{CaEP}/K_a^{CaE}), \qquad (6)$$

per n (2 in our case) number of calcium ions transported per cycle. K_a^{CaE} and K_a^{CaEP} are the *association* constants of the enzyme for Ca^{2+} in the ground state and following activation by ATP. With reference to the reaction scheme given above, the two relevant constants are K_1 and $1/K_5$.

Correction of the standard free energy diagram for the actual concentrations of substrates and products (i.e., ATP, ADP, P_i, Ca^{2+}_{out}, Ca^{2+}_{in}) yields net free energy changes permitting forward or reverse fluxes in general agreement with Eq. 1 (Inesi et al., 1980; Inesi, 1985; Pickart and Jencks, 1984). The advantage of this analysis is to be mechanistically explicit, and to spell out the specifications of the transport "machine." It makes clear that, although the pump is in principle capable of establishing a transmembrane gradient commensurate with the free energy of the coupled substrate (as predicted by Eq. 1), in fact it will be limited by kinetic constraints to the concentration ranges dictated by the binding constants of the enzyme in the high and low affinity states. For instance, the same pump will operate ideally raising a gradient from the micromolar to the millimolar range (Fig. 3), but much less competently from the nanomolar to the micromolar range, or from the millimolar to the molar range. The pump will be also able to synthesize ATP in the presence of millimolar Ca^{2+}_{in} and < micromolar Ca^{2+}_{out}, given a proper [ATP]/([ADP][P_i]) ratio, as observed experimentally. The importance of "machine" specifications in extracting useful work from the potential energy of a substrate can be stressed mundanely by pointing out that a motorcycle will not fly even if provided with high energy aviation fuel, as may be implied by Eq. 1.

With regards to the electrogenic characteristics of the SR Ca^{2+} pump and their physiological implications we can reason as follows: 1) A transmembrane potential is formed when the pump is reconstituted in proteoliposomes of low permeability (as explained above), but is not likely to be maintained when the pump is in the native SR membrane due to the presence of channels permitting electrolyte diffusion and charge compensation. 2) It can be shown in the reconstituted system that a transmembrane potential (up to 40 mV) has little effect on the kinetics of the pump, suggesting that the rate-limiting step of the catalytic and transport cycles is not rate-limiting. 3) From the thermodynamic standpoint it can be calculated that active countertransport of 2 H^+ and 2 Ca^{2+} ions against an electrical potential of 40 mV requires a free energy expenditure of 1.8 Kcal, as compared to 8.5 or 11.3 Kcal required to move 2 mol of calcium against a concentration gradient of three or four orders of magnitude. In conclusion, even though the interesting experiments with reconstituted systems demonstrate the intrinsic electrogenicity

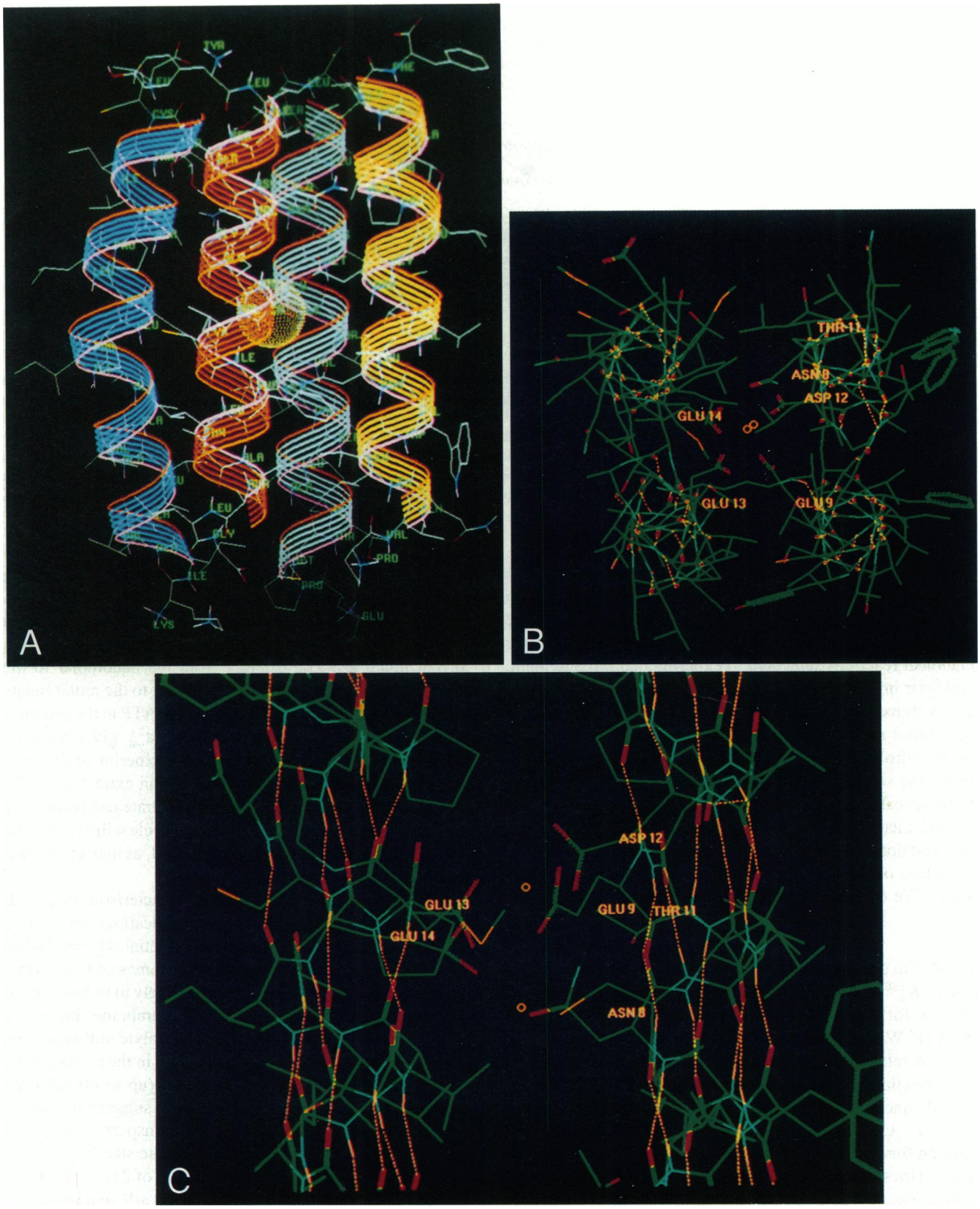

FIGURE 6 Molecular graphics study of a putative Ca^{2+} binding domain within four clustered transmembrane helices. The anphiphylic transmembrane helices M4, M5, M6, and M8, containing the six residues involved in Ca^{2+} binding function, are here clustered with their polar side chains facing a narrow channel. (*A*) The four helical segments are shown with their entire membrane spanning length, and are bent due to the presence of proline residues in their sequences. The van der Waals sphere of a calcium ion is shown as a yellow ball in the center of the channel at the position where it would be complexed by the six binding residues side chains. (*B*) A transversal section of the channel is viewed from the cytosolic end. The helices, starting from lower left,

of the Ca^{2+} pump mechanism, at present there is no evidence that this is likely to place a major limit to the function of the SR Ca^{2+} pump *in situ*.

Structural features of transport enzymes

The very nature of their function implies that transport enzymes are membrane-bound proteins, capable of coupling catalytic activity with transfer of specific ligands across the membrane and against a concentration gradient. With specific reference to our example, shape and topology of the SR ATPase were revealed by electron microscopy and diffraction experiments (Stokes and Green, 1990), and consist of a globular cytosolic region connected by a stalk to a membrane bound region (Fig. 4).

The amino acid sequence of the SR ATPase and several isoforms was obtained from cloned cDNAs, allowing analysis of homologies among the isoforms and other transport ATPases. The distribution of the ATPase polypeptide chain in and out of the membrane bilayer can also be predicted with some approximation, based on segmental hydrophobicity indices within the amino acid sequence. It is then predicted (MacLennan et al., 1985) and supported by immunological localization of specific epitopes, that 10 helical segments span the membrane bilayer forming five hairpins going in and out of the bilayer, and leaving a large and a smaller segment, as well as the amino and carboxyl terminals, protruding from the cytosolic side of the membrane bilayer (Fig. 5). Furthermore, spectroscopic experiments and structural modeling have contributed valuable suggestions on the three-dimensional folding of cytosolic and membrane bound regions of the ATPase. Presentation of transport ATPase structures in the teaching setting yields wonderful opportunities for references to cloning and sequencing methods, as well as to methods of protein structural analysis.

Location of the catalytic domain within the ATPase cytosolic region

Several transport ATPases, including the Ca^{2+} pump, utilize ATP by accepting its terminal phosphate to form a phosphorylated intermediate, as outlined in the reaction sequence given above. Identification of the aspartyl residue undergoing phosphorylation yields the first lead for localization of the phosphorylation site. Furthermore, evidence derived from chemical derivatization and site-directed mutagenesis indicates that the entire catalytic domain, comprising phosphorylation and ATP binding sites, resides within the cytosolic globular region of the ATPase. Analogies with nucleotide handling kinases, whose crystal structure is known, suggest that the three-dimensional folding of the ATPase cytosolic region includes two hinged globular domains permitting approximation of bound nucleotide to the phosphoryl transfer site upon enzyme activation (Green et al., 1986).

Approximate distances separating fluorescent labels placed as spectroscopic reference points within the folded structure of the cytosolic region were obtained from resonance energy transfer (Fig. 5). Consideration of these distances suggests a trigonal arrangement for approximation of various peptide segments within the cytosolic region, and their interaction with adenine, ribose, and phosphate moieties of bound ATP. Diffraction studies and triangulation of spectroscopic distances indicate that the cytosolic region containing the catalytic domain is an elongated globular structure of approximately 40 × 50 × 65-Å dimensions, connected to the membrane-bound region by a stalk of 16-Å length and 28-Å diameter. Estimates of the distance between a Lys^{515} label (likely at the upper end of the cytosolic region) and the membrane surface is approximately 60 Å. Most importantly, the distance between the phosphorylation site (Asp^{351}) and the membrane surface is approximately 40 Å. Fluorescence (Bigelow and Inesi, 1992) and paramagnetic spectroscopy (Thomas et al., 1993) provide very useful means for structural studies of the Ca^{2+} transport ATPase and other functional proteins.

Location of the Ca^{2+} binding domain within the ATPase membrane-bound region

As implied by the reaction sequence given above, another important functional domain relates to cation binding and translocation. The SR ATPase binds with high affinity two Ca^{2+} which are responsible for enzyme activation. The mechanism of binding is cooperative and involves sequential binding in a protein crevice permitting positioning of the two bound Ca^{2+} in a single file with alternate exposure to cytosolic and lumenal sides of the membrane vesicles, as revealed by isotope exchange experiments. Recent experimental evidence produced by site-directed mutagenesis, chemical derivatization, and chimeric recombination of Ca- and Na,K-ATPases, indicates that Ca^{2+} binding occurs within the membrane-bound region of the enzyme. In fact, six amino acids (Glu^{309}, Glu^{771}, Asn^{796}, Thr^{799}, Asp^{800}, and Glu^{908}) within the putative membrane spanning segments 4, 5, 6, and 8 of the ATPase polypeptide chain, have been identified as residues participating in Ca^{2+} complexation (Clarke et al., 1989a). Molecular modeling indicates that the four helical segments 4, 5, 6, and 8 can be clustered within the

are M4, M5, M6, and M8. The residues involved in Ca^{2+} binding are Glu^{9} (Glu^{771} in the ATPase sequence), Glu^{13} (Glu^{309} in the ATPase sequence), Glu^{14} (Glu^{908} in the ATPase sequence), Asn^{8} (Asn^{796} in the ATPase sequence), Thr^{121} (Thr^{799} in the ATPase sequence) and Asp^{12} (Asp^{800} in the ATPase sequence). Helix 6 (which contains Asn^{8}, Thr^{11}, and Asp^{12}) can either be positioned with Asp^{8} and Asp^{12} coordinating Ca^{2+} (as shown here) or it can be rotated to bring Thr^{11} close to Ca^{2+}. (*C*) An enlarged longitudinal view of a duplex Ca^{2+} binding site is modeled after the duplex Ca^{2+} binding described in the crystal structure of thermolysin (Holmes and Matthews, 1982). Three Glu residues (9, 13, and 14) coordinate both Ca^{2+}. The upper Ca^{2+} is coordinated with Asp^{12}, while the lower Ca^{2+} coordinates with Asp^{8}. Helix 6 (which contains Asn^{8}, Thr^{12}, and Asp^{12}) is positioned to optimize participation of Asp^{8} and Asp^{12} (Inesi et al., 1993).

membrane to form a narrow channel, and rotated to optimize participation of the six residues in Ca^{2+} complexation (Fig. 6). In fact, there are sufficient oxygen functions provided by the six residues along the central surface of the four helix channel (Inesi et al., 1993) to coordinate two Ca^{2+} using either of the coordination numbers, 6 (octahedral) and 7 (pentagonal bipyramidal), commonly seen in Ca^{2+} binding sites of proteins. A relevant example of cooperative binding of two Ca^{2+} in close proximity to each other is found in the crystal structure of thermolysin where two of the bound Ca^{2+} are 3.8 Å apart: the first site is heptacoordinate with pentagonal bipyramidal geometry, the second is hexacoordinate with octahedral geometry, and three acidic side chains are shared by both Ca^{2+}.

Coupling of substrate utilization and ligand translocation

A fundamental question regarding the coupling mechanism is whether the transmission of forces between chemical groups undergoing catalytic transfer and cations undergoing vectorial translocation is direct and short range, or indirect and long range. An example of short range transmission is the phosphate-cation symport hypothesis, assuming a direct interaction of the phosphoryl group undergoing transfer and cations undergoing translocation. However, experimental evidence obtained through mutagenesis, chemical derivatization, and spectroscopy indicates that catalytic and Ca^{2+} binding domains are separated by a distance of approximately 50 Å, thereby requiring a long range linkage. It is likely that the long range linkage of catalytic and translocation events is accomplished by minor, but extended changes of protein conformation, as suggested by a number of experimental observations. The peptide segment connecting the phosphorylation domain in the extramembranous region with the Ca^{2+} binding domain within the membrane bound region, retains a surprising degree of homology in all cation transport ATPases, and may have a prominent role in the coupling mechanism. In fact, we find that the ATP function is highly sensitive to single mutations of several residues within this segment (Zhang et al., 1993). Precise definition of the long range coupling mechanism remains a challenge for the very few years separating us from the twenty-first century.

I am indebted to Drs. Joel Cohen and Mary Kirtley for criticisms and suggestions.

This article is derived from a lecture given at the 2nd International Union of Biochemistry and Molecular Biology Conference on the Biochemistry of Cell Membranes, 1993. Support by the National Institutes of Health, American Heart Association and National Science Foundation is gratefully acknowledged.

REFERENCES

Bigelow, D. J., and G. Inesi. 1992. Contributions of chemical derivatization and spectroscopic studies to the characterization of the Ca^{2+} transport ATPase of sarcoplasmic reticulum. *Biochim. Biophys. Acta Bio-Membr.* 1113:323–338.

Clarke, D. M., T. W. Loo, G. Inesi, and D. H. MacLennan. 1989a. Location of high affinity Ca^{2+}-binding sites within the predicted transmembrane domain of the sarcoplasmic reticulum Ca^{2+}-ATPase. *Nature (Lond.).* 339:476–478.

Clarke, D. M., K. Maruyama, T. W. Loo, E. Leberer, G. Inesi, and D. H. MacLennan. 1989b. Functional consequences of glutamate, aspartate, glutamine, and asparagine mutations in the stalk sector of the Ca^{2+}-ATPase of sarcoplasmic reticulum. *J. Biol. Chem.* 264:11246–11251.

Dupont, Y., S. Harrison, and W. Hasselbach. 1973. Molecular organization in the sarcoplasmic reticulum membrane studied by x-ray diffraction. *Nature (Lond.).* 244:554–558.

Green, N. M., W. R. Taylor, C. J. Brandl, B. Korczak, and D. H. MacLennan. 1986. Structural and mechanistic implications of the amino acid sequence of calcium transporting ATPases. *CIBA Foundation Symp.* 122:93–114.

Hasselbach, W. 1964. Relaxing Factor and the relaxation of muscle. *Prog. Biophys. Biophys. Chem.* 14:169–222.

Holmes, M. A., and B. W. Matthews. 1982. Structure of thermolysin refined at 1:6 Å resolution. *J. Mol. Biol.* 160:623–639.

Inesi, G. 1979. Transport across sarcoplasmic reticulum in skeletal and cardiac muscle. *In* Membrane Transport in Biology. G. Giebisch, D. Tosteson, and H. Ussing, editors. Springer-Verlag, Berlin, Heidelberg. 357–393.

Inesi, G. 1985. Mechanism of calcium transport. *Annu. Rev. Physiol.* 47: 573–601.

Inesi, G., M. Kurzmack, C. Coan, and D. Lewis. 1980. Cooperative calcium binding and ATPase activation in sarcoplasmic reticulum vesicles. *J. Biol. Chem.* 255:3025–3031.

Inesi, G., M. Kurzmack, and D. Lewis. 1988. Kinetic and equilibrium characterization of an energy-transducing enzyme and its partial reactions. *Methods Enzymol.* 157:154–190.

Inesi, G., M. Kurzmack, and S. Verjovski-Almeida. 1978. ATPase phosphorylation and calcium ion translocation in the transient state of sarcoplasmic reticulum activity. *Ann. NY Acad. Sci.* 307:224–227.

Inesi, G., L. Lu, and M. E. Kirtley. 1994. Distinct structural identities of catalytic and Ca^{2+} binding domains in the sarcoplasmic reticulum ATPase. *Cell Physiol. Biochem.* 4:135–147.

Lauger, P. 1993. Electrogenic Ion Pumps. Sinauer Associates, Sunderland, MA.

Levy, D., M. Seigneuret, A. Bluzat, and J. L. Rigaud. 1990. Evidence for proton countertransport by the sarcoplasmic reticulum Ca^{2+}-ATPase during calcium transport in reconstituted proteoliposomes with low ionic permeability. *J. Biol. Chem.* 265:19524–19534.

MacLennan, D. H., C. J. Brandl, B. Korczak, and N. M. Green. 1985. Amino-acid sequence of a $Ca^{2+}+Mg^{2+}$ dependent ATPase from rabbit muscle sarcoplasmic reticulum, deduced from its complementary DNA sequence. *Nature (Lond.).* 316:696–700.

Pickart, C., and W. P. Jencks. 1984. Energetics of the calcium-transporting ATPase. *J. Biol. Chem.* 259:1629–1643.

Stokes, D. L., and N. M. Green. 1990. Structure of CaATPase: electron microscopy of frozen-hydrated crystals at 6 Å resolution in projection. *J. Mol. Biol.* 213:529–538.

Thomas, D. D., E. M. Ostap, C. L. Berger, S. M. Lewis, P. G. Fajer, and J. E. Mahaney. 1993. EMR of paramagnetic molecules. *In* Biological Magnetic Resonance. L. J. Berliner and J. Reuben, editors. Plenum Press, New York. pp. 323–351.

Toyoshima, C., H. Sasabe, and D. L. Stokes. 1993. Three-dimensional cryo-electron microscopy of the calcium ion pump in the sarcoplasmic reticulum membrane. *Nature (Lond.).* 362:469–471.

Zhang, Z., C. Sumbilla, D. Lewis, and G. Inesi. 1993. High sensitivity to site directed mutagenesis of the peptide segment connecting phosphorylation and Ca^{2+}-binding domains in the Ca^{2+} transport ATPase. *FEBS Lett.* 335:261–264.